Clinical Cancer Research

New Strategies in Prostate Cancer: Prostate-Specific Membrane Antigen (PSMA) Ligands for Diagnosis and Therapy

Uwe Haberkorn[1,2], Matthias Eder[3], Klaus Kopka[3], John W. Babich[4], and Michael Eisenhut[1,3]

Abstract

Key issues for prostate cancer patients are the detection of recurrent disease and the treatment of metastasized cancer. Early detection is a major challenge for all conventional imaging modalities. Furthermore, therapy of patients with hormone-resistant tumor lesions presents a major clinical challenge. Because the prostate-specific membrane antigen (PSMA) is frequently overexpressed in prostate cancer, several PSMA-targeting molecules are under development to detect and treat metastatic castration-resistant prostate cancer (mCRPC). mCRPC represents a situation where cure is no longer achievable and novel therapeutic approaches for palliation and increase of survival are needed. In this article, we discuss the recent development for noninvasive detection of recurrent disease and therapy of mCRPC with corresponding PSMA-targeted radioligands. *Clin Cancer Res; 22(1); 9–15. ©2016 AACR.*

Disclosure of Potential Conflicts of Interest

U. Haberkorn reports receiving a commercial research grant from Molecular Insight Pharmaceuticals (now Progenics Pharmaceuticals). J.W. Babich was an employee of Molecular Insight Pharmaceuticals. No potential conflicts of interest were disclosed by the other authors.

Editor's Disclosures

The following editor(s) reported relevant financial relationships: J.L. Abbruzzese is a consultant/advisory board member for Celgene and Halozyme.

CME Staff Planners' Disclosures

The members of the planning committee have no real or apparent conflicts of interest to disclose.

Learning Objectives

Upon completion of this activity, the participant should be able to understand the background and pharmacokinetics of PSMA ligands for PET/CT, estimate the value of PSMA-based imaging in comparison to choline-based imaging, assess the value of PSMA targeting for diagnosis and therapy, and estimate the effects and side effects of endoradiotherapy with PSMA ligands.

Acknowledgment of Financial or Other Support

This activity does not receive commercial support.

Background

Prostate cancer is the most common cancer in men in Europe and the United States. Early detection of localized disease results in a 5-year survival rate of nearly 100%. However, metastasized tumors lead to dramatically reduced survival rates. Early detection not only leads to a decrease in mortality, but also to overdiagnosis and overtreatment, which has a negative impact on the quality of life of men with prostate cancer (1). The variability of clinical course and high prevalence of microscopic disease (2, 3) create the need for risk-adapted strategies to optimize patient care. These strategies cover a whole spectrum from active surveillance to aggressive treatment. In that respect patient-adapted staging is essential for better individual outcomes and requires sensitive and specific imaging of prostate cancer, including intraprostatic disease as well as local and distant metastases. Furthermore, if active surveillance becomes a management option in low-grade disease, a sensitive method of monitoring changes in tumor volume, location, and aggressiveness would potentially eliminate the need for repetitive biopsies, thereby enabling a more advanced temporal evaluation *in vivo*.

[1]Department of Nuclear Medicine, University Hospital Heidelberg, Heidelberg, Germany. [2]Clinical Cooperation Unit Nuclear Medicine, German Cancer Research Center (dkfz), Heidelberg, Germany. [3]Division of Radiopharmaceutical Chemistry, German Cancer Research Center (dkfz), Heidelberg, Germany. [4]Department of Radiopharmacy, Weill Cornell Medical College, New York, New York

Corresponding Author: Uwe Haberkorn, University Hospital Heidelberg, Im Neuenheimer Feld 400, Heidelberg 69120, Germany. Phone: 49-6221-567731; Fax: 49-6221-565473; E-mail: uwe.haberkorn@med.uni-heidelberg.de

doi: 10.1158/1078-0432.CCR-15-0820

Prostate-specific antigen (PSA) kinetics has been used so far to assess the risk in first-line treatment failures, but the method is known to be unreliable for active surveillance (4), because even a stable PSA during the first 2 years after diagnosis does not preclude the formation of distant metastases and the possibility of lethal cancer (5–7).

Because distinct changes at the molecular level are responsible for the biologic behavior of tumors, trials to validate biomarkers that identify patients at risk are under way. Genomics data may lead to a better prediction of tumor behavior; however, it still has not achieved widespread acceptance, because biopsies are required (3). In contrast, noninvasive imaging offers the possibility to perform repeated measurements of tumor progression and biologic alteration, which can be used for individual patient staging and guiding the optimal treatment option. In essence, monitoring changes in disease burden at the whole-body level may offer the best means of patient management.

PET/CT with choline tracers has been widely used for the staging and detection of recurrent disease; however, numerous studies report a low sensitivity and specificity of these tracers, especially in patients with low PSA levels (8–11). Consequently, improved imaging of prostate cancer is necessary. One novel promising method is PET imaging with anti-1-amino-3-[^{18}F]fluorocyclobutane-1-carboxylic acid (^{18}F-FACBC), a new synthetic amino acid. Recent evaluations by Nanni and colleagues present evidence that this tracer is superior when compared with choline-PET/CT (12). However, there is still a high demand for novel imaging and therapy procedures targeting structures associated with aggressive disease, which could improve the detection rate and offer options for the treatment of metastatic disease, especially in the case of metastatic castration-resistant prostate cancer (mCRPC). Because curative approaches no longer exist for patients with mCRPC and also the use of androgen receptor axis-targeted drugs, such as abiraterone and enzalutamide, inevitably leads to resistance against these agents, new isotope-based pharmaceuticals offer the chance of symptom relief and/or prolongation of survival.

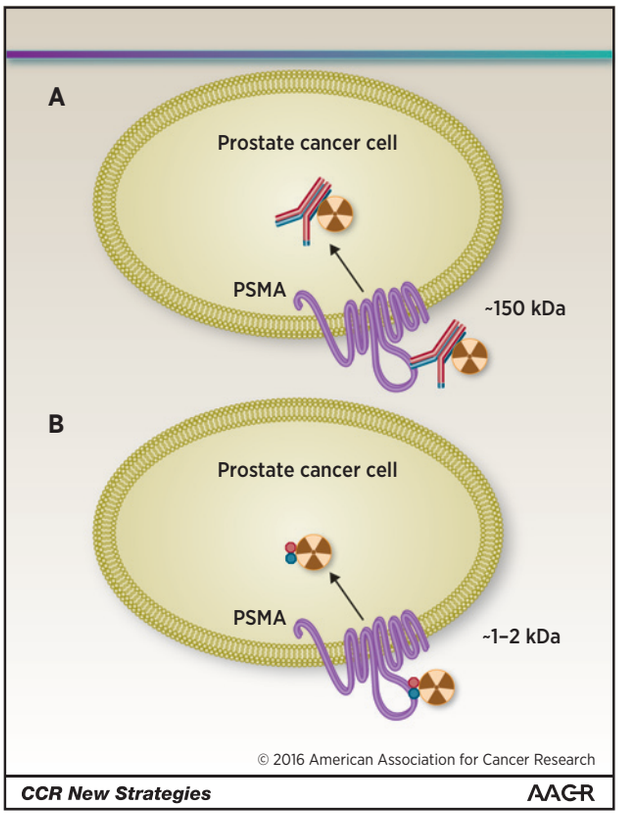

Figure 1.
After binding to PSMA, the ligand (A, antibody; B, small molecule) is internalized into the cell. Because the clearance of small molecules is very fast, this leads to an excellent contrast during the first 60 minutes after injection of the molecule.

On the Horizon

Prostate-specific membrane antigen as a target

Several biologic characteristics make prostate-specific membrane antigen (PSMA), also known as folate hydrolase I or glutamate carboxypeptidase II, an outstanding target for drug development. PSMA is a type II transmembrane protein with glutamate-carboxypeptidase activity and shows a significant overexpression on prostatic cancer cells, including advanced-stage prostate carcinomas (13, 14), but a low expression in normal tissues. Thus, PSMA can be considered as ideal for developing small and low-molecular-weight targeted radiopharmaceuticals with fast blood clearance and low background activity. Furthermore, upon ligand binding PSMA is internalized via clathrin-coated pits and subsequent endocytosis (15), resulting in an effective transportation of the bound molecule into the cells. This leads to an enhanced uptake, deposit, and retention in the tumor, resulting in high image quality for diagnosis and a high local dose for therapeutic applications (Fig. 1). Several studies report that PSMA expression levels increase according to the stage and grade of the tumor (14–17). Moreover, nearly all adenocarcinomas of the prostate show PSMA expression in the majority of primary and metastatic lesions (17, 18). Therefore, a variety of PSMA-targeted radioligands for diagnosis and therapy has been developed (see selected refs. 19–43). Table 1 summarizes selected radiopharmaceuticals for the diagnosis and therapy of prostate cancer.

Diagnostics

Clinical trials with the radiolabeled anti-PSMA monoclonal antibody J591 have shown improved targeting of prostate cancer (41, 43). Although antibodies offer potential for tumor targeting, their effectiveness as diagnostic radiopharmaceuticals is limited by a long biologic half-life and poor tumor penetrability, particularly for bone metastases. There are promising approaches that may overcome these limitations, such as combining antibodies with the longer-lived PET radionuclides ^{89}Zr and ^{64}Cu (42) or using single chain fragments or the anti-PSMA minibody ^{89}Zr-Df-IAB2M as smaller variants of the humanized J591. Apart from diagnosis, however, antibodies directed against PSMA may have an adjuvant therapeutic impact as they are able to recruit cells of the immune system.

Early work on the development of small molecule inhibitors, mimicking the endogeneous substrate *N*-acetyl-L-aspartyl-L-glutamate (NAAG), normally cleaved by *N*-acetylated alpha-linked acidic dipeptidase (NAALADase) or glutamate carboxy-peptidase II, identified a number of candidates as described by several groups (44–46). Ultimately, the identification of the structural

Table 1. Radiopharmaceuticals used for diagnosis and therapy of prostate cancer

Tracer	Principle	Application
^{18}Fluorodeoxyglucose	Glucose metabolism	Diagnosis, PET
^{11}C-acetate	Fatty acid *de novo* synthesis	Diagnosis, PET
^{11}C-choline, ^{18}F-choline, ^{18}F-methylcholine, ^{18}F-ethylcholine	Phospholipid biosynthesis	Diagnosis, PET
^{18}F-FACBC	Amino acid transport; synthetic leucine analogue	Diagnosis, PET
^{111}In-J591	PSMA ligand; antibody	Diagnosis, SPECT
^{64}Cu-J591	PSMA ligand; antibody	Diagnosis, PET
^{89}Zr-J591	PSMA ligand; antibody	Diagnosis, PET
^{99m}Tc-MIP-1404	PSMA ligand; small-molecule inhibitor	Diagnosis, SPECT
^{123}I-MIP-1072, ^{123}I-MIP-1095	PSMA ligand; small-molecule inhibitor	Diagnosis, SPECT
^{18}F-DCFBC	PSMA ligand; small-molecule inhibitor	Diagnosis, PET
^{68}Ga-PSMA-HBED-CC (PSMA-11)	PSMA ligand; small-molecule inhibitor	Diagnosis, PET
^{90}Y-J591	PSMA ligand; antibody	Therapy
^{177}Lu-J591	PSMA ligand; antibody	Therapy
^{131}I-MIP-1466	PSMA ligand; small-molecule inhibitor	Therapy
^{177}Lu-PSMA-617	PSMA ligand; small-molecule inhibitor	Therapy

Abbreviation: SPECT, single photon emission computed tomography.

and functional (47, 48) homology between NAALADase and PSMA opened the prospect of using these small molecules in the targeted treatment and imaging of prostate cancer. Subsequent to these reports several groups have reported on the development of small-molecule inhibitors of PSMA labeled with ^{123}I, ^{99m}Tc, ^{18}F, ^{111}In, and ^{68}Ga, based on the structural motifs of various NAALADase inhibitors (25–37, 39, 49, 50).

The first high-affinity small-molecule inhibitors of PSMA, ^{123}I-MIP-1072, and ^{123}I-MIP-1095, were introduced into the clinic in 2008. In men with metastatic prostate cancer, SPECT/CT using these molecules demonstrated the ability to rapidly detect lesions in soft tissue, bone, and the prostate gland as early as 1 to 4 hours after injection (30). ^{123}I-MIP-1072 was subsequently evaluated in an animal model of prostate cancer under chemotherapy and clearly demonstrated that tumor uptake is directly proportional to the viable tumor mass, providing the potential to track changes in response to therapy.

Glu-NH-CO-NH-Lys-(Ahx)-[^{68}Ga(HBED-CC)] (^{68}Ga-PSMA-11) as a ^{68}Ga-labeled PSMA-targeted radioligand became one of the most successful radiopharmaceuticals with respect to on-site availability (32) and clinical application. In a retrospective analysis in 319 patients, at least one lesion was detected in 82.8% of the patients (33). Tumor detection was positively associated with PSA level and androgen deprivation therapy. Gleason score and PSA doubling time (PSA-DT) were not associated with tumor detection. Among lesions investigated by histology, 30 were false-negative in 4 different patients, and all other lesions ($n = 416$) were true-positive or true-negative. A lesion-based analysis of sensitivity, specificity, negative predictive value, and positive predictive value revealed values of 76.6%, 100%, 91.4%, and 100%, respectively. A patient-based analysis revealed a sensitivity of 88.1%; among 116 patients available for follow-up, 50 received local therapy after ^{68}Ga-PSMA-ligand PET/CT. These data were confirmed by a study done in 248 patients (51), in which 89.5% of the patients had pathologic findings. The detection rates in this study were 96.8%, 93.0%, 72.7%, and 57.9% for PSA levels of $\geq$2, 1 to <2, 0.5 to <1, and 0.2 to <0.5 ng/mL, respectively. Furthermore, the detection rates increased with a higher PSA velocity (81.8%, 82.4%, 92.1%, and 100% in <1, 1 to <2, 2 to <5, and $\geq$5 ng/mL/y, respectively), but no significant association could be found for PSA-DT (51). In 70 patients, factors associated with the outcome of ^{68}Ga-PSMA-ligand PET/CT were studied. ^{68}Ga-PSMA-ligand PET/CT was positive in 74.2%. PSA level ($P = 0.017$) and PSA doubling time ($P = 0.0001$) were significantly different between PET-positive patients (higher PSA level, shorter PSA-DT) and PET-negative patients (lower PSA, longer PSA-DT). A ROC analysis showed that a PSA-DT of 6.5 months and a PSA of 0.83 ng/mL were optimal cut-off values (52).

A comparison of ^{18}F-fluoromethylcholine- and ^{68}Ga-PSMA-ligand PET/CT in 37 patients with biochemical relapse of prostate cancer (mean PSA 11.1 $\pm$ 24.1 ng/mL; range 0.01–116; median 4.0) showed that 78 prostate cancer–suspicious lesions were detected in 32 patients using ^{68}Ga-PSMA-ligand PET/CT and 56 lesions were detected in 26 patients using choline-PET/CT. The higher detection rate in ^{68}Ga-PSMA-ligand PET/CT concerning prostate cancer–suspicious lesions was significant ($P = 0.04$). All lesions detected by ^{18}F-fluoromethylcholine-PET/CT were also seen by ^{68}Ga-PSMA-ligand PET/CT. In ^{68}Ga-PSMA-ligand, PET/CT SUV_{max} was clearly (>10%) higher in 62 of 78 lesions (79.1%) and tumor-to-background ratio was clearly (>10%) higher in 74 of 78 lesions (94.9%) when compared with ^{18}F-fluoromethylcholine-PET/CT. Therefore, ^{68}Ga-PSMA-PET/CT detects prostate cancer–suspicious relapses and metastases with improved contrast when compared with standard ^{18}F-fluoromethylcholine-PET/CT, especially at low PSA levels (31).

Up to now, a systematic analysis of PSMA ligand PET/CT performance in patients with primary tumors prior to standardized surgery and standardized pathologic evaluation has not been done. Such an analysis would result in reliable data concerning the sensitivity and specificity of PSMA ligand imaging for tumor and lymph node metastasis detection.

Treatment

Theranostics in endoradiotherapy: see what you treat. Given that a cell surface associated molecule is overexpressed in the tumor compared with normal tissues, therapeutically active doses can be delivered to the target tissue with diminished side effects. Depending on the radionuclide used radiolabeled drugs additionally allow imaging. The attractive feature is that patients may first be identified as possible candidates for endoradiotherapy after labeling of the carrier molecule with a γ or positron emitter. Upon positive findings, the same molecule can be used for therapy by labeling it with an α- or β-particle emitter. Further advantages of endoradiotherapy over traditional therapies can be expected from the cross-fire effect induced by the β particles originating from the binding site. These particles lead to the destruction of multiple

cells in the neighborhood of the target-expressing cell and may compensate for heterogeneous target expression in tumors. These results are in contrast to nonradioactive targeting treatment, where usually only the cells binding the therapeutic molecule are destroyed. Further enhancement of therapeutic effects is caused by the radiation-induced bystander effect (RIBE). RIBE describes a situation where cells, which have not been directly exposed to the ionizing radiation, behave as if they have been exposed: they die or show chromosomal instabilities or other abnormalities. Although the exact mechanism of RIBE is not fully understood, there is evidence that chemical signaling processes transmit information from irradiated cells to neighboring cells (53).

PSMA-targeted radioimmunotherapy. J591 is a second-generation mAb that recognizes the extracellular portion of PSMA. J591 has been the subject of several clinical studies using various radionuclides. Both ^{90}Y- or ^{177}Lu-labeled J591 have been the focus of independent phase I trials in men with mCRPC (20–24).

In the ^{90}Y-J591 phase I trial (21), 29 patients received therapeutic doses of 5, 10, 15, 17.5, and 20 mCi/m^2 ^{90}Y-J591. Dose-limiting toxicity was seen at 20 mCi/m^2, with 2 patients experiencing thrombocytopenia with non–life-threatening bleeding episodes requiring platelet transfusions. The 17.5-mCi/m^2 dose level was determined to be the maximum tolerated dose (MDT). Two patients treated at the 20-mCi/m^2 dose level exhibited 85% and 70% declines in PSA lasting 8 and 8.6 months, respectively, prior to returning to pretreatment values. In addition, these 2 patients had objective measurable disease responses with 90% and 40% decrease in the size of pelvic and retroperitoneal lymphadenopathy. In 6 patients, PSA stabilization was observed by week 12.

In the ^{177}Lu-J591 phase I trial, 35 patients received J591 radiolabeled with doses of ^{177}Lu ranging from 10 mCi/m^2 to 75 mCi/m^2 (22). Of the 3 patients at the 75-mCi/m^2 dose level, 1 experienced dose-limiting (grade 4) thrombocytopenia and 1 experienced dose-limiting neutropenia that lasted for 6 days. The 70-mCi/m^2 dose level was determined to be the MTD. Retreatment was allowed after hematologic recovery. Repeated dosing at 45 to 60 mCi/m^2 6 to 12 weeks after the initial dose resulted in dose-limiting myelosuppression; up to 3 doses of 30 mCi/m^2 could be safely administered. Based on PSA criteria, 14 patients showed progressive disease (PSA increase of $\geq$25%) after treatment whereas 21 of 35 patients had evidence of biologic activity. Four patients had $\geq$50% PSA declines lasting 3+ to 8 months, and 16 patients had PSA stabilization (<25% increase from baseline) lasting at least 28 days. The median duration of PSA stabilization was 60 days, with a range of 28 to 601 days.

Subsequently, a dual-center phase II study of the safety and efficacy of ^{177}Lu-J591 was performed in 47 patients with progressive mCRPC (24). Fifteen patients received 65 mCi/m^2, and 17 received 70 mCi/m^2. All patients experienced reversible hematologic toxicity, with grade 4 thrombocytopenia occurring in 46.8% (29.8% received platelet transfusions) without significant hemorrhage; 25.5% experienced grade 4 neutropenia with 1 episode of febrile neutropenia. The phase I MTD (70 mCi/m^2) resulted in more than 30% PSA declines (46.9% vs. 13.3%, $P = 0.048$) and longer survival (21.8 vs. 11.9 months, $P = 0.03$), but also more grade 4 hematologic toxicity and platelet transfusions. No serious nonhematologic toxicity occurred. Overall, 59.6% of the patients experienced any PSA decline following their single treatment, with 36.2% experiencing a $\geq$30% decline and 10.6% experiencing a $\geq$50% decline in PSA.

Therapy with PSMA inhibitors. The results of the initial clinical investigation of ^{123}I-MIP-1072 and ^{123}I-MIP-1095 led to the evaluation of these radioiodinated ligands as potential PSMA-targeted radiotherapeutics when radiolabeled with ^{131}I (25,26,30).

Dosimetry scans were done in 16 patients with ^{124}I-MIP-1095 PET/CT (54). Based on the biodistribution data obtained from the ^{124}I-MIP-1095 PET images, the absorbed dose for ^{131}I-MIP-1095 was calculated using the physical decay characteristics of ^{131}I (software OLINDA/EXM). The organs receiving the highest absorbed doses following administration of ^{131}I-MIP-1095 are the salivary glands [mean dose 4.6 mGy/MBq, followed by the liver (1.5 mGy/MBq) and the kidneys (1.5 mGy/MBq)]. This leads to an estimated absorbed dose for the injected therapy activities (mean dose 4.8 GBq, range 2.0–7.2 GBq) for the salivary glands of 9.2 to 33.3 Gy. Liver radiation doses fall in the range of 2.9 to 10.6 Gy. The kidneys received a total absorbed dose between 2.9 and 10.4 Gy. The mean total whole-body absorbed dose was 0.38 mGy/MBq resulting in 0.76 to 2.7 Gy based on the injected activities. Lymph node and bone metastases were exposed to estimated absorbed doses up to 300 Gy (54).

Therapy was done in 25 men with mCRPC, which demonstrated PSMA-avid lesions on imaging. The patients received a single therapeutic activity of ^{131}I-MIP-1095 (mean activity 4.8 GBq, range 2.0–7.2 GBq). In 14 patients, white blood cell counts fell below the normal range after therapy (10 patients with grade 1, 3 with grade 2, and 1 with grade 3 toxicity). However, 5 of these 14 patients had levels below normal prior to therapy (4 grade 1, 1 grade 2). Erythrocyte counts fell below the normal range at nadir in 21 patients, with 17 patients having lower values prior to therapy. With respect to platelets, 11 patients had a reduction in counts below normal after therapy (8 grade 1, 1 grade 2, and 2 grade 3), and 1 had a value below normal (grade 2) prior to therapy. The changes in hematologic parameters were not related to the activity administered. The onset of the myelosuppression occurred within 6 weeks after treatment with a quite variable time to recovery, in some cases requiring up to 3 to 6 months for recovery. White blood cells typically recovered within several weeks, whereas platelets required several months to recover.

In some patients, evidence of nonhematologic transient side effects was found: 7 patients reported having a slight to moderate xerostomia and in 1 patient mucositis was detected. All reported recovery from side effects after 3 to 4 weeks. This latter finding is likely due to the high level of radiopharmaceutical accumulation in these organs and the estimated absorbed doses.

After treatment, 3 out of 13 (23.1%) patients with bone pain reported complete resolution of bone pain, and 8 (61.5%) reported a decrease in pain severity. In the remaining 2 patients the outcome is unknown. In 60.7% of patients a decline in serum PSA levels of $\geq$50% was observed; 7 (25%) had more than a 75% drop in PSA, 10 (35.7%) had a drop between 50% and 75%, 2 (7.1%) between 25% and 50%, and 2 (7.1%) between 0% and 25% (54). One patient showed a long-lasting complete response by serum PSA value and by radiographic imaging. In 4 patients an increase of PSA was observed. As with the hematologic parameters, the changes in PSA value were not related to the activity administered. In the 19 patients showing a more than 25% decrease in PSA, the median time to PSA progression was 126

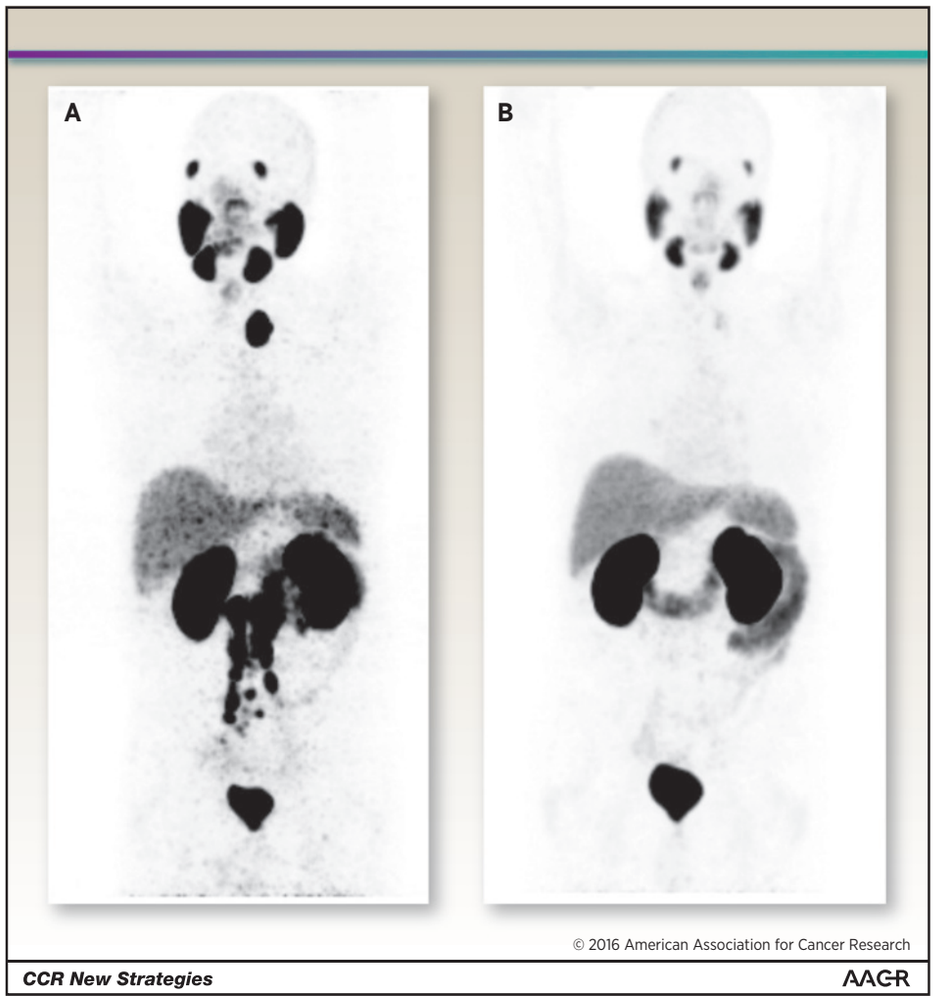

Figure 2.
PET/CT images [maximal intensity projection (MIP) images, image reconstruction was done using an ordered subset expectation maximization algorithm with 4 iterations/8 subsets to an in-plane spatial resolution of 3 mm at full-width at half-maximum] obtained with a Siemens Biograph 6 after administration of 180 MBq ^{68}Ga-PSMA-11 prior (A) and after (B) two cycles with ^{131}I-labeled MIP-1095. The PET images show a reduction in tumor mass.

days (range 62–469 days). A decrease in PSA was associated with a decrease in number and/or intensity of the lesions visualized on the posttherapeutic PET/CT scan with ^{68}Ga-labeled Glu-NH-CO-NH-Lys(Ahx)-HBED-CC (PSMA11; Fig. 2).

Although ^{131}I-MIP-1095 confirms that this class of PSMA inhibitors may be effective for radiotherapeutic applications, the use of β-particle emitting radionuclides such as ^{177}Lu or ^{90}Y would be preferable, given the advantages of energy, availability, and the potential for on-site labeling via kit formulations. To that end, PSMA inhibitors have been developed, which include chelators for labeling with radiometals commonly used for radiodiagnostic and radiotherapeutic applications. The most potent DOTA-conjugates of PSMA inhibitors exhibit affinity constants which compare favorably with the compounds that already have entered the clinic and shown excellent tumor uptake and retention. The versatility of DOTA facilitates the use of β-emitters, such as ^{177}Lu and ^{90}Y, and α-emitters, such as ^{225}Ac, with minimal γ emissions that can be readily and safely used in the clinic (49, 55, 56).

Authors' Contributions

Conception and design: U. Haberkorn, J.W. Babich, M. Eisenhut
Development of methodology: J.W. Babich, M. Eisenhut
Analysis and interpretation of data (e.g., statistical analysis, biostatistics, computational analysis): U. Haberkorn
Writing, review, and/or revision of the manuscript: U. Haberkorn, M. Eder, K. Kopka, J.W. Babich, M. Eisenhut
Study supervision: U. Haberkorn

Grant Support

U. Haberkorn was supported by a grant from the Klaus Tschira Foundation (00.198.2012). M. Eder was supported by a grant from the Deutsche Forschungsgemeinschaft (ED234/2-1).

Received April 2, 2015; revised August 25, 2015; accepted August 30, 2015; published online January 4, 2016.

References

1. Resnick MJ, Koyama T, Fan KH, Albertsen PC, Goodman M, Hamilton AS, et al. Long-term functional outcomes after treatment for localized prostate cancer. N Engl J Med 2013;368:436–45.
2. Pinto F, Totaro A, Palermo G, Calarco A, Sacco E, D'Addessi A, et al. Imaging in prostate cancer staging: present role and future perspectives. Urol Int 2012;88:125–36.

3. Klotz L. Cancer overdiagnosis and overtreatment. Curr Opin Urol 2012; 22:203–9.
4. Ross AE, Loeb S, Landis P, Partin AW, Epstein JI, Kettermann A, et al. Prostate-specific antigen kinetics during follow-up are an unreliable trigger for intervention in a prostate cancer surveillance program. J Clin Oncol 2010;28:2810–6.
5. Lees K, Durve M, Parker C. Active surveillance in prostate cancer: patient selection and triggers for intervention. Curr Opin Urol 2012;22:210–5.
6. Loblaw A, Zhang L, Lam A, Nam R, Mamedov A, Vesprini D, et al. Comparing prostate specific antigen triggers for intervention in men with stable prostate cancer on active surveillance. J Urol 2010;184:1942–6.
7. Fall K, Garmo H, Andren O, Bill-Axelson A, Adolfsson J, Adami HO, et al. Prostate-specific antigen levels as a predictor of lethal prostate cancer. J Natl Cancer Inst 2007;99:526–32.
8. Schmid DT, John H, Zweifel R, Cservenyak T, Westera G, Goerres GW , et al. Fluorocholine PET/CT in patients with prostate cancer: initial experience. Radiology 2005;235:623–8.
9. Igerc I, Kohlfurst S, Gallowitsch HJ, Matschnig S, Kresnik E, Gomez-Segovia I , et al. The value of ^{18}F-Choline PET/CT in patients with elevated PSA-level and negative prostate needle biopsy for localisation of prostate cancer. Eur J Nucl Med Mol Imaging 2008;35:976–83.
10. Husarik DB, Miralbell R, Dubs M, John H, Giger OT, Gelet A , et al. Evaluation of [^{18}F]-Choline PET/CT for staging and restaging of prostate cancer. Eur J Nucl Med Mol Imaging 2008;35:253–63.
11. Cimitan M, Bortolus R, Morassut S, Canzonieri V, Garbeglio A, Baresic T , et al. ^{18}F-fluorocholine PET/CT imaging for the detection of recurrent prostate cancer at PSA relapse: experience in 100 consecutive patients. Eur J Nucl Med Mol Imaging 2006;33:1387–98.
12. Nanni C, Schiavina R, Boschi S, Ambrosini V, Pettinato C, Brunocilla E , et al. Comparison of ^{18}F-FACBC and ^{11}C-choline PET/CT in patients with radically treated prostate cancer and biochemical relapse: preliminary results. Eur J Nucl Med Mol Imaging 2013;40:S11–7.
13. Perner S, Hofer MD, Kim R, Shah RB, Li H, Moller P, et al. Prostate-specific membrane antigen expression as a predictor of prostate cancer progression. Hum Pathol 2007;38:696–701.
14. Silver DA, Pellicer I, Fair WR, Heston WD, Cordon-Cardo C. Prostate-specific membrane antigen expression in normal and malignant human tissues. Clin Cancer Res 1997;3:81–5.
15. Rajasekaran SA, Anilkumar G, Oshima E, Bowie JU, Liu H, Heston W, et al. A novel cytoplasmic tail MXXXL motif mediates the internalization of prostate-specific membrane antigen. Mol Biol Cell 2003;14:4835–45.
16. Chang SS. Overview of prostate-specific membrane antigen. Rev Urol 2004;6:S13–8.
17. Bostwick DG, Pacelli A, Blute M, Roche P, Murphy GP. Prostate specific membrane antigen expression in prostatic intraepithelial neoplasia and adenocarcinoma: a study of 184 cases. Cancer 1998;82:2256–61.
18. Mannweiler S, Amersdorfer P, Trajanoski S, Terrett JA, King D, Mehes G. Heterogeneity of prostate-specific membrane antigen (PSMA) expression in prostate carcinoma with distant metastasis. Pathol Oncol Res 2009; 15:167–72.
19. Smith-Jones PM, Vallabahajosula S, Goldsmith SJ, Navarro V, Hunter CJ, Bastidas D, Bander NH. *In vitro* characterization of radiolabeled monoclonal antibodies specific for the extracellular domain of prostate-specific membrane antigen. Cancer Res 2000;60:5237–43.
20. Vallabhajosula S, Goldsmith SJ, Kostakoglu L, Milowsky MI, Nanus DM, Bander NH. Radioimmunotherapy of prostate cancer using ^{90}Y- and ^{177}Lu-labeled J591 monoclonal antibodies: effect of multiple treatments on myelotoxicity. Clin Cancer Res 2005;11:7195s-200s.
21. Milowsky MI, Nanus DM, Kostakoglu L, Vallabhajosula S, Goldsmith SJ, Bander NH. Phase I trial of yttrium-90-labeled anti-prostate-specific membrane antigen monoclonal antibody J591 for androgen-independent prostate cancer. J Clin Oncol 2004;22:2522–31.
22. Bander NH, Milowsky MI, Nanus DM, Kostakoglu L, Vallabhajosula S, Goldsmith SJ. Phase I trial of ^{177}lutetium-labeled J591, a monoclonal antibody to prostate-specific membrane antigen, in patients with androgen-independent prostate cancer. J Clin Oncol 2005;23:4591–601.
23. Vallabhajosula A, Goldsmith SJ, Hamacher KA, Kostakoglu L, Konishi S, Milowski MI, et al. Prediction of myelotoxicity based on bone marrow radiation-absorbed dose: radioimmunotherapy studies using ^{90}Y- and ^{177}Lu-labeled J591 antibodies specific for prostate-specific membrane antigen. J Nucl Med 2005;46:850–8.
24. Tagawa ST, Milowsky MI, Morris M, Vallabhajosula S, Christos P, Akhtar NH, et al. Phase II study of lutetium-177 labeled anti-prostate-specific membrane antigen (PSMA) monoclonal antibody J591 for metastatic castration-resistant prostate cancer. Clin Can Res 2013;19:5182–91.
25. Maresca KP, Hillier SM, Femia FJ, Keith D, Barone C, Joyal JL, et al. A series of halogenated heterodimeric inhibitors of prostate specific membrane antigen (PSMA) as radiolabeled probes for targeting prostate cancer. J Med Chem 2009;52:347–57.
26. Hillier SM, Maresca KP, Femia FJ, Marquis JC, Foss CA, Nguyen N, et al. Preclinical evaluation of novel glutamate-urea-lysine analogues that target prostate-specific membrane antigen as molecular imaging pharmaceuticals for prostate cancer. Cancer Res 2009;69:6932–40.
27. Hillier SM, Maresca KP, Lu G, Merkin RD, Marquis JC, Zimmerman CN, et al. ^{99m}Tc-labeled small-molecule inhibitors of prostate-specific membrane antigen for molecular imaging of prostate cancer. J Nucl Med 2013;54:1369–76.
28. Lu G, Maresca KP, Hillier SM, Zimmerman CN, Eckelman WC, Joyal JL, Babich JW. Synthesis and SAR of ^{99m}Tc/Re-labeled small molecule prostate specific membrane antigen inhibitors with novel polar chelates. Bioorg Med Chem Lett 2013;23:1557–63.
29. Eder M, Schafer M, Bauder-Wust U, Hull WE, Wangler C, Mier W, et al. ^{68}Ga-Complex lipophilicity and the targeting property of a urea-based PSMA inhibitor for PET imaging. Bioconjugate Chem 2012;23:688–697.
30. Barrett JA, Coleman RE, Goldsmith SJ, Vallabhajosula S, Petry NA, Cho S, et al. First-in-man evaluation of two high-affinity PSMA-avid small molecules for imaging prostate cancer. J Nucl Med 2013;54:380–7
31. Afshar-Oromieh A, Zechmann CM, Malcher A, Eder M, Eisenhut M, Linhart HG, et al. Comparison of PET imaging with a ^{68}Ga-labelled PSMA-ligand and ^{18}F-choline based PET/CT for the diagnosis of recurrent prostate cancer. Eur J Nuc Med Mol Imaging 2014;41:11–20.
32. Eder M, Neels O, Müller M, Bauder-Wüst U, Remde Y, Schäfer M, et al. Novel preclinical and radiopharmaceutical aspects of [^{68}Ga]Ga-PSMA-HBED-CC: a new PET tracer for imaging of prostate cancer. Pharmaceuticals (Basel) 2014;7:779–96.
33. Afshar-Oromieh A, Avtzi E, Giesel FL, Holland-Letz T, Linhart HG, Eder M, et al. The diagnostic value of PET/CT imaging with the ^{68}Ga-labelled PSMA ligand HBED-CC in the diagnosis of recurrent prostate cancer. Eur J Nucl Med Mol Imaging 2015;42:197–209.
34. Eder M, Eisenhut M, Babich J, Haberkorn U. PSMA as a target for radiolabelled small molecules. Eur J Nucl Med Mol Imaging 2013;40:819–23.
35. Afshar-Oromieh A, Malcher A, Eder M, Eisenhut M, Linhart HG, Hadaschik BA, et al. PET imaging with a [^{68}Ga]gallium-labelled PSMA ligand for the diagnosis of prostate cancer: biodistribution in humans and first evaluation of tumour lesions. Eur J Nucl Med Mol Imaging 2013;40:486–95.
36. Cho SY, Gage KL, Mease RC, Senthamizhchelvan S, Holt DP, Jeffrey-Kwanisai A, et al. Biodistribution, tumor detection, and radiation dosimetry of ^{18}F-DCFBC, a low-molecular-weight inhibitor of prostate-specific membrane antigen, in patients with metastatic prostate cancer. J Nucl Med 2012;53:1883–91.
37. Szabo Z, Mena E, Rowe SP, Plyku D, Nidal R, Eisenberger MA, Antonarakis ES, et al. Initial evaluation of ^{18}F-DCFPyL for prostate-specific membrane antigen (PSMA)-targeted PET imaging of prostate cancer. Mol Imaging Biol 2015;17:565–74.
38. Banerjee SR, Pullambhatla M, Foss CA, Nimmagadda S, Ferdani R, Anderson CJ, et al. Cu-labeled inhibitors of prostate-specific membrane antigen for PET imaging of prostate cancer. J Med Chem 2014;57:2657–69.
39. Banerjee SR, Pullambhatla M, Foss CA, Falk A, Byun Y, Nimmagadda S, et al. Effect of chelators on the pharmacokinetics of ^{99m}Tc-labeled imaging agents for the prostate-specific membrane antigen (PSMA). J Med Chem 2013;56:6108–21.
40. Herrmann K, Bluemel C, Weineisen M, Schottelius M, Wester HJ, Czernin J, et al. Biodistribution and radiation dosimetry for a probe targeting prostate-specific membrane antigen for imaging and therapy. J Nucl Med 2015;56:855–61.
41. Evans MJ, Smith-Jones PM, Wongvipat J, Navarro V, Kim S, Bander NH, et al. Noninvasive measurement of androgen receptor signaling with a positron-emitting radiopharmaceutical that targets prostate-specific membrane antigen. Proc Natl Acad Sci U S A 2011;108:9578–82.
42. Holland JP, Divilov V, Bander NH, Smith-Jones PM, Larson SM, Lewis JS. ^{89}Zr-DFO-J591 for immunoPET of prostate-specific membrane antigen expression in vivo. J Nucl Med 2010;51:1293–300.

43. Morris MJ, Divgi CR, Pandit-Taskar N, Batraki M, Warren N, Nacca A, et al. Pilot trial of unlabeled and indium-111-labeled anti-prostate-specific membrane antigen antibody J591 for castrate metastatic prostate cancer. Clin Cancer Res 2005;11:7454–61.
44. Jackson PF, Slusher BS. Design of NAALADase inhibitors: a novel neuroprotective strategy. Curr Med Chem 2001;8:949–57.
45. Liu T, Toriyabe Y, Kazak M, Berkman CE. Pseudoirreversible inhibition of prostate-specific membrane antigen by phosphoramidate peptidomimetics. Biochemistry 2008;47:12658–60.
46. Kozikowski AP, Zhang J, Nan F, Petukhov PA, Grajkowska E, Wroblewski JT, et al. Synthesis of urea-based inhibitors as active site probes of glutamate carboxypeptidase II: efficacy as analgesic agents. J Med Chem 2004; 47:1729–38.
47. Tiffany CW, Lapidus RG, Merion A, Calvin DC, Slusher BS. Characterization of the enzymatic activity of PSM: comparison with brain NAALADase. Prostate 1999;39:28–35.
48. Mesters JR, Barinka C, Li W, Tsukamoto T, Majer P, Slusher BS, et al. Structure of glutamate carboxypeptidase II, a drug target in neuronal damage and prostate cancer. EMBO J 2006;25:1375–84.
49. Benes?ová M, Schäfer M, Bauder-Wüst U, Afshar-Oromieh A, Kratochwil C, Mier W, et al. Preclinical evaluation of a tailor-made DOTA-conjugated PSMA inhibitor with optimized linker moiety for imaging and endoradiotherapy of prostate cancer. J Nucl Med 2015;56:914–20.
50. Chen Y, Pullambhatla M, Foss CA, Byun Y, Nimmagadda S, Senthamizhchelvan S, et al. 2-(3-{1-Carboxy-5-[(6-[^{18}F]fluoro-pyridine-3-carbonyl)-amino]-pentyl}-ureido)-pentanedioic acid, [^{18}F]DCFPyL, a PSMA-based PET imaging agent for prostate cancer. Clin Cancer Res 2011;17:7645–53.
51. Eiber M, Maurer T, Souvatzoglou M, Beer AJ, Ruffani A, Haller B, et al. Evaluation of hybrid ^{68}Ga-PSMA ligand PET/CT in 248 patients with biochemical recurrence after radical prostatectomy. J Nucl Med 2015;56:668–74.
52. Ceci F, Uprimny C, Nilica B, Geraldo L, Kendler D, Kroiss A, et al. ^{68}Ga-PSMA PET/CT for restaging recurrent prostate cancer: which factors are associated with PET/CT detection rate? Eur J Nucl Med Mol Imaging 2015;42:1284–94.
53. Haberkorn U, Eisenhut M, Altmann A, Mier W. Endoradiotherapy with peptides—status and future development. Curr Med Chem 2008; 15:219–34.
54. Zechmann CM, Afshar-Oromieh A, Armor T, Stubbs JB, Mier W, Hadaschik B, et al. Radiation dosimetry and first therapy results with a ^{124}I/^{131}I-labeled small molecule (MIP-1095) targeting PSMA for prostate cancer therapy. Eur J Nucl Med Mol Imaging 2014;41:1280–92.
55. Kratochwil C, Giesel FL, Eder M, Afshar-Oromieh A, Benes?ová M, Mier W, et al. [^{177}Lu]Lutetium-labelled PSMA ligand-induced remission in a patient with metastatic prostate cancer. Eur J Nucl Med Mol Imaging 2015;42:987–8.
56. Kratochwil C, Giesel FL, Leotta K, Eder M, Hoppe-Tich T, Youssoufian H, et al. PMPA for nephroprotection in PSMA-targeted radionuclide therapy of prostate cancer. J Nucl Med 2015;56:293–8.